

***This is the accepted version of the following article:***

***T. Soriano, J.I. Montero, M.C. Sánchez-Guerrero, E. Medrano, A. Antón, J. Hernández, M.I. Morales, N. Castilla, A Study of Direct Solar Radiation Transmission in Asymmetrical Multi-span Greenhouses using Scale Models and Simulation Models, Biosystems Engineering, Volume 88, Issue 2, 2004, Pages 243-253***

***which has been published in final form at:***

***<https://doi.org/10.1016/j.biosystemseng.2004.03.006>***

1 **A Study of Direct Solar Radiation Transmission in Asymmetrical**  
2 **Multi-span Greenhouses using Scale Models and Simulation**  
3 **Models**

4  
5 T. Soriano<sup>1</sup> ; J.I. Montero<sup>2</sup> ; M.C. Sanchez-Guerrero<sup>3</sup> ; E. Medrano<sup>3</sup> ; A. Anton<sup>2</sup> ;  
6 J. Hernandez<sup>4</sup> ; M.I. Morales<sup>1</sup> ; N. Castilla<sup>1</sup>

7  
8 <sup>1</sup> CIFA, Apartado 2027, 18080 Granada, Spain; e-mail:ncastil@arrakis.es

9 <sup>2</sup> IRTA, Carretera de Cabrils, s/n 08348 Barcelona, Spain; e-mail of  
10 corresponding author: [juanignacio.montero@irta.es](mailto:juanignacio.montero@irta.es)

11 <sup>3</sup>CIFA, Apartado 91. El Ejido, 04700 Almería, Spain; e-mail: fisiovht@arrakis.es

12 <sup>4</sup> University of Almería, La Canada de San Urbano, 04120 Almería, Spain; e-mail:  
13 jhrodri@ual.es

14  
15  
16 **Abstract**

17 Direct solar radiation transmission inside scale models of greenhouses with  
18 different roof slopes was measured and the results compared with calculations  
19 from a simulation model. Seven different roof slopes were tested, which had  
20 symmetrical and asymmetrical roof shapes: 8°–18°; 18°–8°; 27°–27°; 27°–45°;  
21 36°–55°; 45°–27°; 55°–36° (8°–18° denoting that the south-facing slope was 8°  
22 and the north-facing one was 18°). Radiation transmission in scale models was  
23 quantified using linear solarimeters that integrated solar radiation along the cross-  
24 section of the span. The correlation between measured and calculated hourly and  
25 daily mean transmission values was good. Minor differences were attributed to  
26 the accumulation of dust and condensation on the scale models, two conditions  
27 that were not taken into account in the simulation model.

28 The results of the study showed that direct solar radiation transmission increased  
29 considerably as slope increased, up to a value close to 30°, especially in the  
30 winter months in which radiation was most limited. Assymetrical greenhouses did  
31 not always transmit more than symmetrical ones with similar slopes. In the cases  
32 studied, the scale model with 27-27° symmetrical roof had the highest winter  
33 transmission.

34 The use of scale models allowed different greenhouse structures to be  
35 characterised with respect to direct radiation transmission. This method can  
36 produce considerable savings of time and money and provides a realistic  
37 simulation of radiation transmission in full-scale greenhouses.

38  
39

## 40 **Nomenclature**

- 41  $A$ : absorption by a simple transparent sheet  
42  $C_{abs}$ : power-absorption coefficient,  $m^{-1}$   
43  $D_{MB}$ : mean bias deviation  
44  $D_{RMS}$ : root-mean-square deviation  
45  $E$ : angle between the incident ray and the horizontal axis perpendicular to the  
46 greenhouse span, deg  
47  $E_S$ : standard error  
48  $F$ : reflectance of a single transparent sheet  
49  $L_1$ : south-facing surface of roof, m  
50  $L_2$ : north-facing surface of roof, m  
51  $l_a$ : segment of the beam of radiation that reaches the fourth module of a  
52 greenhouse at gutter height after travelling through the second and third modules  
53 of the same greenhouse, m  
54  $l_b$ : segment of the beam of radiation that reaches the fourth module of a  
55 greenhouse at gutter height after travelling through the first, second and third  
56 modules of the same greenhouse, m  
57  $l_1, l_2$ : portions of the beam of incident light travelling through the first side and the  
58 second side of the roof module  
59  $m$ : number of spans that intercept solar radiation  
60  $N$ : number of simulated or measured data  
61  $N$ : index of refraction  
62  $R_T$ : ratio of measured and calculated daily transmission  
63  $T$ : transmission for a single transparent sheet  
64  $T_{cal}$ : calculated material transmission  
65  $T_D$ : mean daily transmission  
66  $T_{exp}$ : mean daily measured transmission  
67  $T_{LE}$ : lengthwise greenhouse-part transmission  
68  $T_{MAT}$ : cover-material transmission  
69  $T_{meas}$ : measured material transmission  
70  $T_r$ : direct radiation reflected by a greenhouse roof surface and then transmitted  
71  $T_{sim}$ : mean daily simulated transmission  
72  $T_{TE}$ : crosswise greenhouse-part transmission  
73  $T_{TOTAL}$ : total direct radiation transmission  
74  $\alpha$ : slope angle of the south-facing surface of the roof, deg  
75  $\beta$ : slope angle of the north-facing surface of the roof, deg  
76

## 77 1. Introduction

78 One of the advantages of protected cultivation in Mediterranean regions is  
79 the high level of solar radiation that results from the many clear days in autumn  
80 and winter. However, the widespread use of low-cost greenhouses limits the level  
81 of radiation transmitted. Enhanced radiation transmission is regarded as a key  
82 objective for raising production quality and quantity (Cockshull, 1989; Castilla &  
83 López-Gálvez, 1994). Such transmission in greenhouses can be improved by  
84 using carefully designed roof geometry.

85  
86 Various studies on radiation transmission models have been carried out  
87 for sophisticated greenhouses (Bot, 1983; Critten, 1993), but little attention has  
88 been paid to Mediterranean greenhouses. Recently, growers in the south of  
89 Spain have begun to replace old low-cost structures with new greenhouses in an  
90 attempt to increase light transmission in winter months, when produce prices are  
91 higher (Castilla & López-Gálvez, 1994). East–west orientation of saddle-roof  
92 greenhouses in Mediterranean latitudes is better than north–south for maximum  
93 light transmission in autumn and winter, as has been widely reported (Jaffrin &  
94 Urban, 1990; Kurata, 1990; Pieters, 1994; Papadopoulos & Pararajasingham,  
95 1997; Papadakis *et al.*, 1998; Giacomelli & Ting, 1999). There are, however, few  
96 publications on optimal roof slopes (Kozai *et al.*, 1978).

97  
98 When characterising radiation levels in a greenhouse, transmission  
99 through side walls needs to be taken into account. This is particularly true in  
100 single-span greenhouses (Papadakis *et al.*, 1998). However, in large,  
101 commercial multi-span greenhouses, the quantity of radiation received by the  
102 side walls is very small in comparison with the total radiation received by the  
103 greenhouse and it is therefore not necessary to take it into consideration (Bot,  
104 1983).

105  
106 When quantifying radiation transmission, the spatial variability of radiation  
107 in greenhouses makes it necessary for measurements to be taken with spot  
108 sensors in the complete area of one span (Papadakis *et al.*, 1998). When the  
109 variation in the radiation transmitted to different zones of the greenhouse is very  
110 great, or when it is necessary to simultaneously study the transmission of  
111 radiation from several different greenhouses, the number of spot sensors  
112 required may make the job of characterising impractical. Tube solarimeters  
113 integrate radiation data along a line and can provide a representative estimate of  
114 transmission. Tube solarimeters placed on a rotary device have been  
115 successfully used in glasshouses, where shade from structural elements and  
116 equipment can considerably influence radiation transmission (Heuvelink *et al.*,  
117 1995).

118  
119 Mediterranean greenhouses in use in Southern Spain typically have fewer  
120 structural members in the roof, but they also suffer from non-uniform radiation  
121 transmission, due mainly to the different angle of incidence the radiation beam  
122 makes with the different surfaces of the roof. Taking measurements across all  
123 the spans in full-scale Mediterranean greenhouses is a time-consuming task and  
124 requires considerable equipment.

125

126 One approach to solve this problem is using scale models. This method  
127 has been used to quantify the ventilation performance of greenhouses  
128 (Boulard *et al.*, 1998; Oca *et al.*, 1999) and their radiation transmission (Schultz,  
129 1955; Kurata, 1991; Li *et al.*, 1995; Papadakis *et al.*, 1998). Scale models can  
130 also be useful for validating simulation models. In some cases, scale-model  
131 measurements can be considered more representative than simulation models,  
132 because many of the assumptions and simplifications considered in calculations  
133 are avoided by direct measurement under more realistic conditions.

134  
135 The objective of this study was to examine the advantages of using scale  
136 models as a means for studying the transmission of direct radiation in  
137 symmetrical and asymmetrical greenhouses. For this purpose, a number of scale  
138 models of greenhouses with different roof slopes were tested throughout the  
139 year. Tube solarimeters covering all the spans integrated the radiation  
140 transmitted by the greenhouse cover, and actual measurements were compared  
141 with calculations using a simulation model to verify the validity of the scale-model  
142 measurements.

## 143 144 145 **2. Materials and methods**

### 146 **2.1. Scale models**

147 Four saddle-roof multi-span greenhouse models (scale 1:15) were  
148 constructed, oriented east–west and tested at the Agricultural Research and  
149 Development Centre of Granada (CIFA) (latitude 37°10'N) in Southern Spain. To  
150 study all possible cases (Fig. 1, Table 1), the asymmetrical scale models were  
151 rotated 180° during the measuring period, *i.e.* the south-facing roof slope became  
152 north-facing, and vice versa. This was done because there were not enough tube  
153 solarimeters to allow simultaneous readings to be taken for the seven scale  
154 models.

155  
156 Special attention was paid to the evaluation of asymmetrical models, since  
157 they are gaining popularity in Southern Mediterranean areas because of their  
158 potential to increase the solar radiation available for production (Castilla & López-  
159 Gálvez, 1994).

160  
161 Each scale model consisted of three spans, each 110 cm long and 40 cm  
162 wide (representing a 6 m wide, full-scale model, typical of Mediterranean  
163 greenhouses. The length of 110 cm was chosen so that radiation would reach  
164 the sensors, although through the roof and not through the sides). The cover  
165 glass was 8 mm thick and was held in position by a metal support at both ends.  
166 This thickness was chosen to produce a glass sheet rigid enough to avoid the  
167 need for any supporting element along the length of the scale models. The floor  
168 was painted matt black to minimise reflections from the ground.

169  
170 Total solar radiation was measured using tube solarimeters (TSL from  
171 Delta-T). Each sensor covered the full-width of the modules in the central span  
172 and the north span of each model. In this way, it was sought to prevent the  
173 possible entry of solar radiation through the south wall of the scale model and its  
174 incidence on the tube solarimeter. Measurements were taken at the height of the  
175 eaves and at what would have been the height of the gutter in a full-scale

176 greenhouse. Another tube solarimeter was placed in the open air, as was a  
177 pyranometer (Kipp & Zonen, CM6B), which was used for periodic calibration of  
178 the tube solarimeters. Solar radiation data were quantified in 10 min periods  
179 using a data logger (Campbell CR10). Solar radiation transmission was  
180 calculated for half-hour periods and for the whole day during clear-sky conditions  
181 from June 1998 to December 1999. In this study, 30 min periods were considered  
182 due to the need to reduce the volume of data generated by the transmission  
183 measurements and calculations relating to seven types of greenhouse and  
184 different times of the year.

185 An average value for transmission was therefore calculated every 30 min, which  
186 was based on instantly calculated values.

187

188 Regression analysis between measured and calculated transmissions was  
189 carried out for the scale models and for the time periods subject to evaluation  
190 (winter and summer solstices and spring and autumn equinoxes).

191

## 192 **2.2. Transmission model**

193 The transmission model for multi-span greenhouses developed by Bot  
194 (1983) was used to validate measurements taken in scale models. This  
195 transmission model allows for the calculation of direct and diffuse transmission at  
196 any given time. In the Mediterranean, diffuse radiation in sunny days is only a  
197 small part of the global solar radiation. Observations from neighbouring weather  
198 stations indicate that daily diffuse radiation is between 6 and 8% of the total daily  
199 radiation in sunny days. At noon this percentage is even lower. The task of  
200 measuring transmission from the greenhouses to diffused radiation on overcast  
201 days was undertaken at the beginning of this study. It was observed that during  
202 the central hours of the day, the amount of transmission to diffused light on  
203 overcast days was similar to total transmission (direct plus diffused) on sunny  
204 days. Thus, when measuring radiation transmission, the difference between  
205 transmission to direct radiation and to total radiation was only of the order of 1–  
206 2% during the first and last hours of daylight, and insignificant during the middle  
207 hours of the day (Soriano, 2002).

208

209 For the reasons previously cited and for the sake of simplicity, only direct  
210 radiation was considered in this study and therefore only Bot's sub-model for  
211 direct radiation transmission was used. However, Bot's model is not directly  
212 applicable to the calculation of transmission for asymmetrical greenhouses and  
213 its governing equations had to be adapted to cover this case. The adaptation of  
214 the calculating equations is presented in Appendix A.

215

216 The total transmission  $T_{TOTAL}$  is the product of transmission through the  
217 cover material (resulting transmission if there were only covering material without  
218 any kind of structure),  $T_{MAT}$  and transmission through the opaque roof parts,  
219 formed by the lengthwise parts such as the ridge and gutter (resulting  
220 transmission if there were only longitudinal structural elements, without any  
221 covering material or transversal elements),  $T_{LE}$  and the crosswise parts such as  
222 the glazing bars (transmission if there were only transversal structural  
223 elements),  $T_{TE}$ . The total transmission can therefore be written as:

224

225

$$(1) T_{TOTAL} = T_{MAT} T_{LE} T_{TE}$$

226

227

Each component has its own sub-model that takes into account the geometry of the cover and the interaction between neighbouring spans in terms of direct radiation transmission and reflections from one to another.

229

230

231

For the sake of simplicity, the scale models were built without lengthwise or crosswise parts. The ridge in the scale models was formed by leaning one glass pane against another. This created an opaque area (similar to the shadow produced by a bar with a cross section with 8 mm long sides) that was taken into account in the calculation of  $T_{LE}$ . Since there were no transversal structural elements, the value for  $T_{TE}$  could be taken as 1.

232

233

The model was programmed in Fortran to provide transmission according to the position of the sun throughout the day, from dawn to dusk. Instantaneous values were integrated to provide mean daily transmission values.

234

235

236

237

To calculate the transmission of the glazing material as a function of the angle of incidence, the simulation model applied the well-known Fresnel equations. This required prior determination of the index of refraction  $n$  and the power-absorption coefficient  $C_{abs}$  in  $m^{-1}$  that is a measure of the attenuation caused by absorption of solar radiation that results from its passage through the material. In order to do this, the direct radiation transmission of a glass sample was measured using a transmission goniometer developed at Silsoe Research Institute (Kamaruddin, 1999). This apparatus contained a tungsten-halogen lamp with a rotating mirror assembly to vary the angle of incidence of the beam with the glass sample. The angle of incidence was varied from 0 to 90° and the corresponding transmission values were measured. STATGRAPHICS software was then used to determine the best fit between measured transmission values and those calculated using the Fresnel equations, which meant  $n$  and  $C_{abs}$  could be determined (Montero *et al.*, 2001).

238

239

240

241

242

243

244

245

246

247

248

249

250

251

252

253

254

255

### 2.3. Comparison of measurements and calculations

256

257

Two types of comparisons were carried out.

258

259

260

261

262

(1) Mean half-hour transmission values were determined for clear-sky conditions. Linear regressions of measured and calculated values were done for a set of four sunny days for each solstice/equinox (*i.e.* on or around the winter solstice, the summer solstice, the spring equinox and the autumn equinox).

263

264

265

266

267

(2) Mean daily transmission  $T_D$ , for sunny days were measured during a complete annual cycle. For this case, the ratio  $R_T$  of measured  $T_{exp}$  and calculated  $T_{sim}$  daily transmission for each scale model was obtained, as well as the standard error  $E_S$  for each case:

268

269

270

$$(2) R_T = \sum_{i=1}^N (T_{exp,i} / T_{sim,i}) / N$$

271

272

where  $N$  is the number of days for which transmission values were measured or calculated.

273

274

275

$$(3) E_S = \sqrt{\frac{N \sum X^2 - (\sum X)^2}{N(N-1)}}$$

276 where

$$277 \quad (4) X = T_{exp} / T_{sim}$$

278

279 The mean bias deviation  $D_{MB}$  and root-mean-square deviation  $D_{RMS}$  were  
280 also calculated (Foyo-Moreno *et al.*, 2000):

281

$$282 \quad (5) DMB = \frac{1}{N} \sum_{i=1}^N T_{sim,i} - T_{exp,i}$$

283

$$284 \quad (6) DRMS = \frac{1}{N} \sum_{i=1}^N (T_{sim,i} - T_{exp,i})^2$$

285

286

287

## 288 **2.4. Assessment of transmission for different roof slopes**

289 The final task carried out in this study was the comparison of mean daily  
290 transmission for different roof slopes based on the measurements taken in  
291 different greenhouse models.

292

## 293 **3. Results and discussion**

### 294 **3.1. Power-absorption coefficient and index of refraction for the glazing 295 material**

296 The results of laboratory measurements of direct radiation transmission as  
297 a function of the angle of incidence are shown in Fig. 2. As with most materials,  
298 transmission is highest for radiation perpendicular to the plane of the sample and  
299 gradually reduces as the angle of incidence increases. From these measured  
300 values,  $n$  and  $C_{abs}$  were determined from the equations of Fresnel and according  
301 to the procedure developed by Bot (1983). The calculus equations were  
302 programmed on a spreadsheet on which the values of  $n$  and  $C_{abs}$  varied in such  
303 a way as to minimise the difference between the measured  
304 transmission  $T_{meas}$  and the calculated transmission  $T_{cal}$ . The best fit was  
305 obtained with values for  $n$  of 1.6 and  $C_{abs}$  of 5.15. Agreement  
306 between  $T_{meas}$  and  $T_{cal}$  for the given coefficients is shown by the regression line  
307 between them. There was good agreement, as:

308

$$309 \quad (7) T_{means} = 1.0001 T_{cal}$$

310 with a value for the coefficient of determination  $R^2$  of 0.9997.

311

312 These values of  $n$  and  $C_{abs}$  were used for subsequent calculations with the  
313 simulation model.

314

### 315 **3.2. Comparison of mean half-hour transmissions for clear-sky conditions**

316 For the sake of simplicity, only results from the scale model with an 8°  
317 slope on the south-facing side and an 18° slope on the north-facing side (8-18°)  
318 are shown in Fig. 3. Figure 3(a) compares measured and calculated transmission  
319 values for a clear day on or around the winter solstice (13th January), while Fig.  
320 3(b) corresponds to a clear day on or around the summer solstice (19th June).  
321 The mean half-hourly total transmission measured in the scale models was very  
322 close to the simulation results. Nevertheless, the simulation model tended to  
323 produce higher values, the greatest differences being during the hours around  
324 midday, with better agreement at sunrise and sunset.

325



326 Similar differences between transmission at midday and the beginning and  
327 end of the day have been reported previously (Gueymard, 1989; Heuvelink *et al.*,  
328 1995).

329  
330 One possible explanation for the differences in the first half of the day could  
331 be the presence of dust and condensation on the internal side of the glass pane.  
332 While the simulation model assumed 'ideal' conditions, in practice it was  
333 impossible to eliminate these factors completely, despite the efforts made to  
334 reduce them. The higher proportion of diffuse radiation compared with total  
335 radiation at sunrise and sunset due to the low elevation of the sun was not  
336 considered in the simulation model. Diffuse radiation during these periods may  
337 have been responsible for an increase in the measured radiation, which tended  
338 to compensate for the potential reduction in radiation due to the presence of dust  
339 and condensation.

340  
341 Regression coefficients are shown in Table 2, which shows that the slope  
342 of the regression lines for greenhouse models with a low roof angle was always  
343 less than 1.1 and the regression coefficients were close to 0.9. On all dates  
344 except 25th April, as the roof slope increased, the slope of the regression lines  
345 increased as well or remained invariable, which means that agreement between  
346 measurement and simulation was worse. The exception of 25th April may have  
347 been due to an error deriving from the fact that the model does not consider  
348 second degree reflexions, which may be relevant with respect to the total  
349 transmission obtained when slopes are very pronounced. Previous research  
350 (Kurata, 1990) pointed out the importance of second-order reflection in east-west  
351 greenhouses. Schultz (1955) also remarked upon the contribution of the radiation  
352 reflected by the north side of the roof. The maximum difference corresponded to  
353 the greenhouse roof with slopes 27-45° (the south-facing slope was 27° and the  
354 north-facing one was 45°); the predictions from the simulation model for this case  
355 exceeded measurements by 12%.

### 356 357 **3.3. Comparison of mean daily transmission**

358 The trend observed for mean half-hour values also held true for daily  
359 transmission values [Figs 4(a), (b) and (c)]: the predictions from the simulation  
360 model exceeded measurements for all roof slopes under study and for all  
361 seasonal periods considered and differences increased as the roof slope  
362 increased. As shown in Table 3, the calculated mean daily transmission was  
363 approximately 6% higher than that measured for the 8-18° scale model and about  
364 10% higher than that measured for the 27-45° and 36-55° models. This difference  
365 was slightly lower than that found in other models validating transmission in  
366 greenhouses (Baille & Baille, 1990, Li *et al.*, 1995) and was considered  
367 acceptable for the purpose of comparing or designing roof shapes to provide  
368 more efficient radiation transmission. The highest standard errors are also  
369 associated with the scale model with highest slope on the north-facing side (36-  
370 55° and 27-45°).

371  
372 Calculation of the statistical parameters  $D_{MB}$  and  $D_{RMS}$  (Table 4) also  
373 illustrates the tendency of the scale models to systematically produce lower  
374 transmission values than those from the simulation models. Again, the associated  
375 errors were the lowest in the case of the greenhouse with the least slope. An

376 interesting point to be observed in Table 4 is that the  $D_{MB}$  and  $D_{RMS}$  were nearly  
377 the same in the 2 yr of measurements, which is proof of the reliability of the  
378 experimental design.

379

### 380 **3.4. Direct radiation transmission in scale models with different slopes**

381 For the summer solstice, the two models with the gentlest slopes  
382 presented the highest transmission (75% for 18-8° and 71% for 27-27°). This  
383 difference in transmission was not important (offers no practical value for the  
384 growers), however, since shade is usually used to reduce summer radiation in  
385 Mediterranean climates in an attempt to mitigate high temperatures. As autumn  
386 advances, and both the maximum altitude of the sun on the horizon and day  
387 length correspondingly decrease, this situation is inverted. For instance, at the  
388 equinoxes transmission tended to increase as the roof slope increased.  
389 Maximum differences can be found around the winter solstice, when the roof with  
390 the least slope (18-8°) had a transmission power of 59%, while the one with 45-  
391 27° had 66%.

392

393 A case that deserves special attention is the 27-27° symmetrical roof. This  
394 scale model had the highest winter transmission among all the cases compared  
395 in Table 5. This fact can be explained by considering the transmission curve for  
396 glass (Fig. 2), which shows transmission to be nearly constant for angles of  
397 incidence less than approximately 45°. If roof slopes 27-27° and 45-27°N at the  
398 latitude of the experimental site (37°N) are compared, the angle of incidence of  
399 beam radiation for both southern surfaces (27 and 45°) was less than this critical  
400 value of 45° for most of the hours around midday. Their transmission was  
401 therefore almost identical. Nevertheless, the length of the south surface for any  
402 given span width was bigger for the 27° case and, consequently, the amount of  
403 solar energy received along the south surface (and thus transmission through the  
404 south surface) was also greater. Another potential advantage of this symmetrical  
405 roof is uniform transmission throughout the year. According to Table 5, seasonal  
406 variation in transmission was highest for the roof with the least slope (18-8°), and  
407 tended to diminish as roof slope increased.

408

409

## 410 **4. Conclusions**

411 The use of scale models is a valid method for characterising direct-  
412 radiation transmission in greenhouses with different roof angles, since  
413 measurements agreed well with predictions from a simulation model. Better  
414 agreement between measured and simulated values was found for models with  
415 less roof slope.

416

417 For the latitude studied in this article, increased roof slope improved direct  
418 radiation transmission around the time of the winter solstice, up to a certain value  
419 beyond which it once more declined. In summer, however, lower roof angles  
420 corresponded to the highest transmission levels.

421

422 Asymmetrical greenhouses do not necessarily provide greater  
423 transmission than symmetrical ones. An east–west oriented greenhouse with a  
424 roof slope of 27° had the highest transmission of all the models considered in this  
425 study.

426           The use of scale models for studying transmission is a simple and  
427 economical method and can be a useful tool for designing greenhouses with  
428 enhanced radiation transmission.

429

#### 430 **Acknowledgements**

431           This research study was funded by the Ministry of Agriculture and  
432 Fisheries of the Government of Andalusia, the National Institute for Agricultural  
433 and Food Research and Technology (INIA), the Scientific and Technological  
434 Research Centre (CICYT) (research project AGF-96-2512-CO) and the Caja  
435 Rural de Granada savings bank. We would also like to thank the staff of the Silsoe  
436 Research Institute for allowing us to use their transmission goniometer.

437

438

**References**

- 440 Baille M; Baille A (1990). A simple model for the estimation of greenhouse  
441 transmission: influence of structures and internal equipment.  
442 *ActaHorticulturae*, 281, 35–46
- 443 Bot G P A (1983). Greenhouse climate: from physical processes to a dynamic  
444 model. PhD Thesis, University of Wageningen, The Netherlands, 240pp
- 445 Boulard T; Alamrani M; Roy J C; Jaffrin A; Bourden L (1998). Natural ventilation  
446 by thermal effect in a one-half scale model mono-span greenhouse.  
447 *Transactions of the ASAE*, 41(3), 773–781
- 448 Castilla N; Lopez-Galvez J (1994). Vegetable-crop responses in improved low-  
449 cost plastic greenhouses. *Journal of Horticultural Science*, 69(5), 915–921
- 450 Cockshull K E (1989). The influence of energy conservation on crop productivity.  
451 *ActaHorticulturae*, 245, 530–536
- 452 Critten D L (1993). A review of the light transmission into greenhouse crops.  
453 *ActaHorticulturae*, 328, 9–31
- 454 Foyo-Moreno I; Vida J; Olmo F J; Alados-Arboledas L (2000). Estimating solar  
455 ultraviolet irradiance (290–385 nm) by means of spectral parametric models;  
456 SPECTRAL2 and SMARTS2. *Annales Geophysicae*, 18, 1382–1389
- 457 Giacomelli G A; Ting K C (1999). Horticultural and engineering considerations for  
458 the design of integrated greenhouse plant production systems. *Acta*  
459 *Horticulturae*, 481, 475–486
- 460 Gueymard C (1989). An atmospheric transmission model for the calculation of  
461 the clear beam, diffuse and global photosynthetically active radiation.  
462 *Agricultural and Forest Meteorology*, 45, 215–229
- 463 Heuvelink E; Batta L G G; Damen T H J (1995). Transmission of solar radiation  
464 by a multi-span Venlo-type glasshouse: validation of a model. *Agricultural*  
465 *and Forest Meteorology*, 74, 41–59
- 466 affrin A; Urban L (1990). Optimisation of light transmission in modern  
467 greenhouses. *ActaHorticulturae*, 281, 25–33
- 468 Kamaruddin R (1999). A naturally ventilated crop protection structure for tropical  
469 conditions. PhD Thesis, Cranfield University, Silsoe, 204pp
- 470 Kozai T; Goundriaan J; Kimura M (1978). Light transmission and photosynthesis  
471 in greenhouses. Centre for Agricultural Publishing and Documentation,  
472 Wageningen, 99pp
- 473 Kurata K (1990). Role of reflection in light transmission of greenhouses.  
474 *Agricultural and Forest Meteorology*, 52, 319–331
- 475 Kurata K (1991). Scale-model experiments of applying a Fresnel prism to  
476 greenhouse covering. *Solar Energy*, 46, 53–57
- 477 Li S; Kurata K; Takakura T (1995). Solar radiation transmission into a lean to  
478 greenhouse. *Acta Horticulturae*, 399, 127–134
- 479 Montero J I; Anton A; Hernández J; Castilla N (2001). Direct and diffuse light  
480 transmission of insect-proof screens and plastic films for cladding  
481 greenhouses. *Acta Horticulturae*, 559, 203–209
- 482 Oca J; Montero J I; Anton A; Crespo D (1999). A method for studying natural  
483 ventilation by thermal effects in a tunnel greenhouse using laboratory-scale  
484 models. *Journal of Agricultural Engineering Research*, 72, 93–104
- 485 Papadakis G; Manolakos D; Kyritsis S (1998). Solar radiation transmission of a  
486 single-span greenhouse through measurements on scale models. *Journal of*  
487 *Agricultural Engineering Research*, 71, 331–338

488 Papadopoulus A P; Pararajasingham S (1997). The influence of plant spacing on  
489 light interception and use in greenhouse tomato (*Lycopersicum esculentum*  
490 mill.): areview. *Scientia Horticulturae*, 69, 1–29  
491 Pieters J G (1994). Condensation and PAR transmittance of greenhouse.  
492 *Plasticulture*, 112, 23–31  
493 Soriano T (2002). Validación de un modelo de cálculo de transmisividad a  
494 radiación solar directa en invernadero mediante maquetas a escala y  
495 determinación del prototipo óptimo para la costa mediterránea. Validation of  
496 a simulation model for direct solar-radiation transmission in greenhouses  
497 using scale models. Determination of the optimal design for the  
498 Mediterranean coast. PhD dissertation. University of Almería, Spain. 274 pp  
499 Schultz L (1955). Light penetration in glasshouses. Hannover Inst. fur Technik in  
500 Gartenbau und Landwirtschaft der Technischer-Hochschule, Germany



Fig. 1. East–west oriented 1:15 greenhouse models at the experimental site (latitude  $37^{\circ} 10'N$ ), south of Spain, with the south-facing and north-facing slopes shown for each model

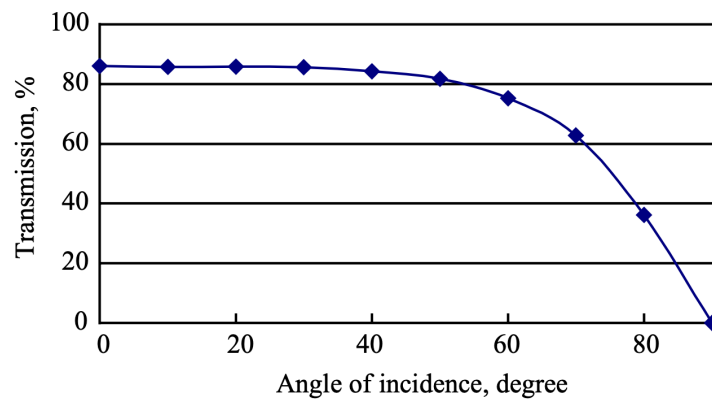


Fig. 2. Laboratory measurement of direct radiation transmission through glass samples as a function of the angle of incidence

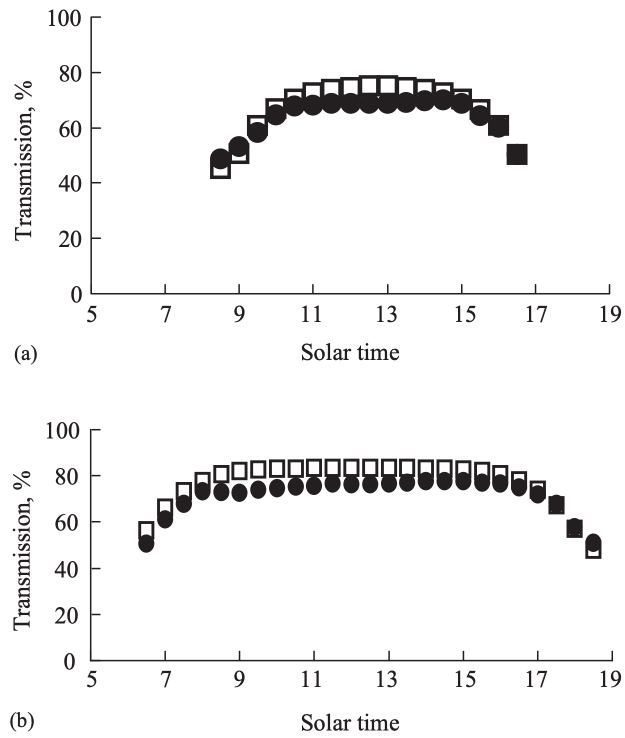


Fig. 3. Comparison of mean half-hour transmission values simulated by the model and measured in the 8-18° scale model (8-18° means that the south-facing slope was 8° and the north-facing one was 18°) on two dates: (a) 13th January; (b) 19th June; measurements taken under clear-sky conditions; □, simulated values; •, measured values

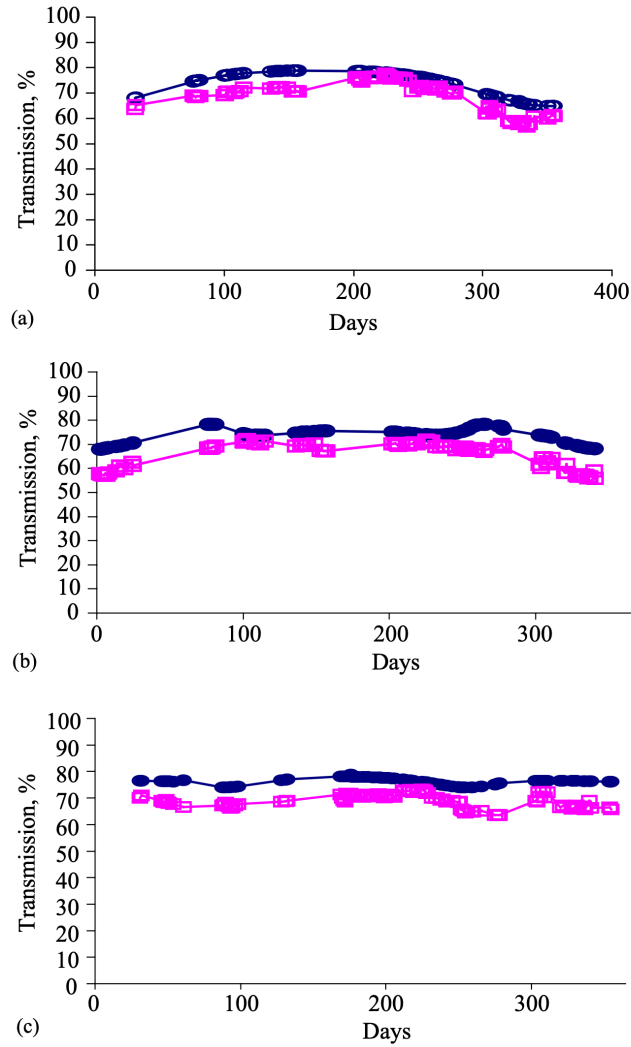


Fig. 4. Comparison of measured and simulated mean daily transmission: (a) 18-8° scale model; (b) 36-55° scale model; (c) 45-27° scale model (18-8° means that the south-facing slope was 18° and the north-facing one was 8°); o, simulated values; □, measured values in scale models



Table 1. Roof slopes of the tested scale models:  $\alpha$  on the south surface and  $\beta$  on the north surface

Scale model	Roof angle, deg	
	South-facing slope ( $\alpha$ )	North-facing slope ( $\beta$ )
1	8	18
2	18	8
3	27	45
4	45	27
5	36	55
6	55	36
7	27	27

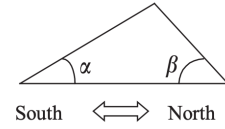


Table 2. Slope of the regression line and regression coefficient between measured and calculated transmission values for the scale models on four clear days

Date	Roof angle, deg		Regression line slope	Regression coefficient
	South-facing slope ( $\alpha$ )	North-facing slope ( $\beta$ )		
13th Jan	8	18	1.05	0.93
	27	45	1.12	0.96
	36	55	1.11	0.76
25th Apr	8	18	1.09	0.87
	27	45	1.1	0.86
	36	55	1.05	0.96
19th Jun	8	18	1.05	0.93
	27	45	1.07	0.87
	36	55	1.07	0.75
16th Sep	8	18	1.02	0.98
	27	45	1.07	0.94
	36	55	1.1	0.82

Table 3. Mean yearly ratio between measured and simulated mean daily transmission for different roof slope models. Standard error of the ratio

<i>Roof angle, deg</i>		<i>Measured transmission / simulated transmission</i>	<i>Standard error</i>
<i>South-facing slope (<math>\alpha</math>)</i>	<i>North-facing slope (<math>\beta</math>)</i>		
8	18	0.94	0.0200
18	8	0.93	0.0197
27	27	0.91	0.0189
27	45	0.90	0.0219
36	55	0.90	0.0432
45	27	0.91	0.0184
55	36	0.92	0.0185

Table 4. Mean bias deviation ( $D_{MB}$ ) in % and root-mean-square deviation ( $D_{RSM}$ ) of the yearly mean of mean daily transmission

<i>Roof angle, deg</i>		<i>Mean bias deviation, %</i>		<i>Root mean square deviation, %</i>	
<i>South-facing slope (<math>\alpha</math>)</i>	<i>North-facing slope (<math>\beta</math>)</i>	<i>1998</i>	<i>1999</i>	<i>1998</i>	<i>1999</i>
8	18	6.9	6.6	7.2	7.7
18	8	7.7	7.9	8.6	8.6
27	27			10	10.4
27	45			12.4	12.7
45	27	10.4	10.5	10.7	11
36	55			12.1	13.4
55	36	8.2	8	8.6	8.2

Table 5. Mean seasonal transmission and maximum differences throughout the year for four roof angle scale models with different roof slopes

<i>Roof angle, deg</i>		<i>Seasonal transmission, %</i>			
<i>South-facing slope (<math>\alpha</math>)</i>	<i>North-facing slope (<math>\beta</math>)</i>	<i>Summer solstice</i>	<i>Equinox</i>	<i>Winter solstice</i>	<i>Maximum difference</i>
18	8	74.9	69.8	59	15.9
36	55	69.7	66.3	56.7	13.0
45	27	71.3	67.7	66.6	4.7
27	27	71	68.5	70.1	0.9